Pathways of bond topology transitions at the interface of silicon nanocrystals and amorphous silica matrix

D. E. Yılmaz[*] and C. Bulutay[†]

Department of Physics, Bilkent University, Ankara 06800, Turkey

T. Çağın[‡]

Artie McFerrin Department of Chemical Engineering, Texas A&M University, Jack E. Brown Engineering Building, 3122 TAMU,
College Station, Texas 77843-3122, USA

The interface chemistry of silicon nanocrystals (NCs) embedded in an amorphous oxide matrix is studied through molecular dynamics simulations with the chemical environment described by the reactive force field model. Our results indicate that the Si NC–oxide interface is more involved than the previously proposed schemes, which were based on solely simple bridge or double bonds. We identify different types of three-coordinated oxygen complexes that are previously not noted. The abundance and the charge distribution of each oxygen complex is determined as a function of the NC size as well as the transitions among them. The oxidation at the surface of NC induces tensile strain to Si—Si bonds, which become significant only around the interface, while the inner core remains unstrained. Unlike many earlier reports on the interface structure, we do not observe any double bonds. Furthermore, our simulations and analysis reveal that the interface bond topology evolves among different oxygen bridges through these three-coordinated oxygen complexes.

I. INTRODUCTION

After a long arduous effort, photoluminescence from silicon has been achieved from its nanocrystalline form.[1] A critical debate, however, continues over the nature of the interface chemistry of silicon nanocrystals (Si NCs) embedded in amorphous silica, which has direct implications on the optical activity of the interface.[2–6] Wolkin *et al.* reported that the oxidation of porous silicon quantum dots results in a redshift in the photoluminescence (PL) spectra, which indicates the importance of oxygen-related interface bond toplogy.[2] Along this line, Puzder *et al.* compared PL calculations of nanoclusters with different passivants and surface configurations and proposed the main reason for the redshift to be double Si=O bonds.[3] Countering this, Luppi *et al.* reported excitonic luminescence features caused by Si—O—Si bridge bonds at the surface of silicon nanoclusters.[4] As a supporting evidence for the latter, Gatti and Onida recently demonstrated that the Si—O—Si bond is the most stable isomer configuration.[5] To reconcile, Vasiliev *et al.* claimed that the bridge bonds and double bonds have similar effects on PL.[6]

All of the work cited above represent density functional theory (DFT)–based calculations with small Si clusters of less than 100 atoms surrounded by either passivants such as hydrogen[3–5] or oxygen.[2,3] However, actual samples are profoundly different: the fabricated systems consist of Si NC with a diameter larger than 1 nm, embedded in an *amorphous* silica (a-SiO$_2$) matrix. Identifying this fact, Tu and Tersoff studied the Si/a-SiO2 interface using a bond order dependent empirical potential and proposed that Si—O—Si bridge bonds are the main blocks at the interface lowering the surface energy.[7] By using the same model potential, Hadjisavvas and Kelires studied Si NCs embedded in a-SiO$_2$ and also reported bridge bonds as the mechanism for lowering surface strain energy.[8] In our previous work on the formation

and structure of Si NCs, we also observed that this model potential falls short in characterizing the system accurately, especially the structure and chemistry at the interface.[9] As a rigorous approach to interface structure and dynamics, Pasquarello *et al.* used first-principles molecular dynamics (MD) technique to investigate the planar Si/SiO$_2$ interface.[10] They observed that the oxygen atoms are momentarily bonded to three silicon atoms during the oxidation process. The net effect of these threefold-coordinated oxygen atoms during the oxidation process was to expel silicon atoms out of the interface. This is interpreted as a balancing process to decrease the increased density of the Si/SiO$_2$ interface due to oxidation.[10] However, no substantial breakthrough was made over the past decade on this issue.

II. METHOD

In this work, we employ the reactive force field (ReaxFF) model developed by van Duin *et al.*,[12] which improves Brenner's reactive bond order model[11] to a level of accuracy and validity, allowing molecular dynamics simulations of the full reaction pathways in bulk. The parameters for this force field were obtained from fitting to the results of *ab initio* calculations on relevant species as well as periodic boundary condition DFT-based calculations of various crystalline polymorphs of relevant materials. The ReaxFF calculates bond orders, which are the measure of bond strength from local geometry. This allows realistic chemical environment such as over- or undercoordination and bond breaking or formation for large-scale (about 5000 atoms) MD simulations.

To facilitate our discussion regarding the surface-bonded oxygen complexes, we distinguish among three different types of silicon atoms. We label those silicon atoms with all silicon neighbors each with zero oxidation state as c to denote core silicon atoms. Among the *remaining* (non-c) sili-
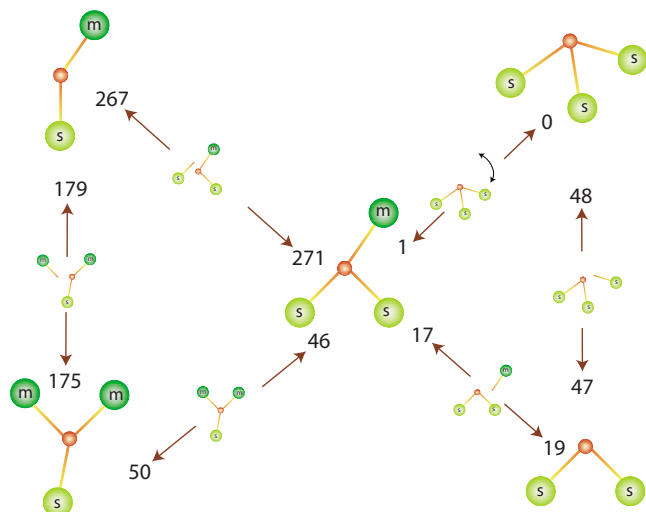
FIG. 1. (Color online) The transitions between different oxygen complexes bonded to the interface. The dark green (dark gray) large spheres represent matrix silicon atoms, the light green (light gray) large spheres represent surface silicon atoms of the NC, and the small red (dark gray) spheres represent oxygen atoms. The numbers indicate the number of transitions recorded in the simulation in each direction among the complexes for the NC with a radius of 13.4 Å.
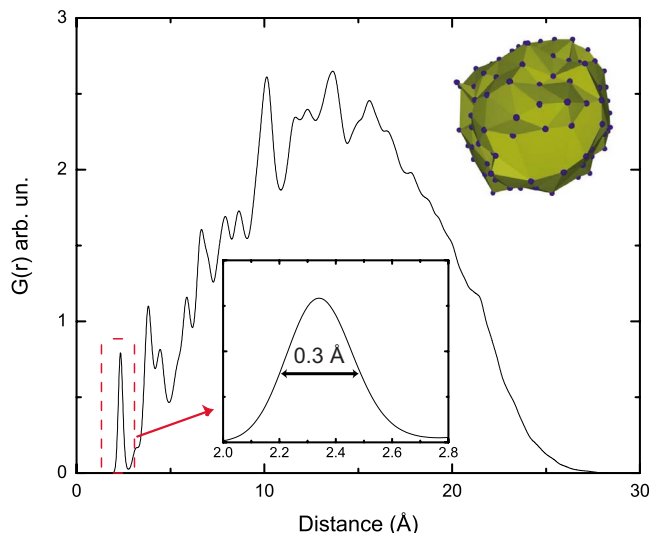

FIG. 2. (Color online) Radial distribution function of Si atoms in NC. Inset: The first peak resembles Si—Si bond length distribution centered at around 2.34 Å with a 0.3 Å FWHM value. The second peak's width resembles bond angle deviation. Inset: Representation of NC surface created with Delaunay triangulation. Blue (dark gray) dots represents surface silicon atoms.

con atoms, those with at least one bond to c are labeled as s, denoting surface silicon atoms. For further investigation of NC, we seperate core Si atoms into two subcategories as inner-core and outer-core atoms: Among core Si atoms which have at least one surface Si neighbor categorized as outer-core Si atoms and rest of core Si atoms categorized as inner-core Si atoms. Finally, any other silicon atom is labeled as m, denoting a matrix silicon atom. Hence, a complex consisting of an oxygen atom bonded with two surface silicon atoms is labeled as ss. The other oxygen complexes are sm, ssm, sss, and mms, as sketched in Fig. 1, where the last three correspond to three-coordinated oxygen (3cO) atoms.

We use ReaxFF to represent the interactions in the model system. We start with a large simulation cell (box length of 43 Å) of silica glass formed through a melting and quenching process used by one of us[13,14] earlier to study silica glasses. Next, similar to Hadjisavvas and Kelires,[8] we delete all atoms within a predetermined radius to insert crystalline silicon to form NC. In this way, we create NCs with radii ranging from 5.5 to 16.7 Å. For the largest NC, we insert 967 Si atoms into a spherical hole with a radius of 16.7 Å created in an amorphous matrix. Even for this case, the minimum distance between the NC surface to the simulation box face is about 5 Å, which can still accommodate the interface layer. We also pay special attention in the removal of spherical region so that the correct stoichiometry for the amorphous matrix is met. Thus, our amorphous matrix has two O atoms for every Si atom with a density of 2.17 g/cm^3, which is the density of glass at room temperature and atmospheric pressure.

We set periodic boundary conditions in all directions, and while keeping NC at 100 K, we employ a simulated annealing process to the SiO$_2$ region to end up with an amorphous matrix free of artificial strain around the NC. Then, we set

the whole systems' temperature to room temperature (300 K) and continue performing MD simulation for 75 ps to have a thermal equilibrium between the two regions. We set the MD simulation time step to 0.25 fs for all simulations. For every 6.25 fs time interval, we have recorded the configurations to analyze the transitions taking place between different bond topologies. The numbers attached to each arrow in Fig. 1 indicate the total number of registered transitions during the simulation in that direction between the complexes for a representative NC with a radius of 13.4 Å. The fact that there are almost balanced rates in opposite directions is an assurance of the attainment of the steady state in our simulation. Note that we do not observe any direct transition other than the paths indicated in Fig. 1. For instance, a direct transition of the complex ss to sm does not take place, but it is possible through an intermediate transition over the ssm, which is a 3cO. We should also remark that the balanced transitions continue to take place after the steady state is attained, which indicates that the interface bond topology is dynamic, i.e., not frozen.

To analyze the Si NC/a-SiO$_2$ interface, we construct a NC surface using the Delaunay triangulation scheme (Fig. 2 inset).[15] In two dimensions, a Delaunay triangulation of a set of points corresponds to defining triangles such that no point in the set is inside the circumcircle of any triangle. In three dimensions, triangles extend to tetrahedra and circumcircles become circumspheres. Since our NCs are nearly spherical in shape, we triangulate projection points of surface Si atoms onto the unit sphere. Hence, we apply Delaunay triangulation over the two dimensional θ-ϕ plane. We can then create surfaces using this triangulation. This surface enables us to calculate every atoms' distance to the NC surface. By this means, we plot various data such as charge, bond order, etc., with respect to distance to the surface to extract information
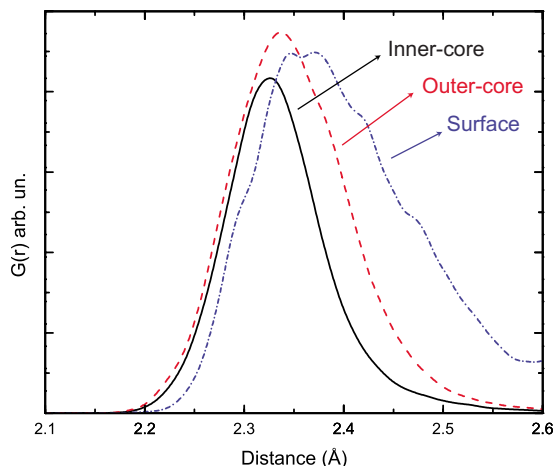
FIG. 3. (Color online) Bond distance probability distribution of Si atoms in NC. The solid line represents inner-core Si—Si bonds, the dashed line outer-core Si—Si bonds, and the dotted line surface Si—Si bonds.

about the surface chemistry of Si NC embedded in amorphous matrix.

III. RESULTS AND DISCUSSIONS

For different NC radii, we observe similar trends in bond order distribution, average charges, etc.; therefore, we present only the figures of the system for a typical NC of radius 13.4 Å. Useful data to elucidate the structure of these systems are the radial distribution function (RDF). In Fig. 2, we present the RDF of NC atoms only, where the first broad peak centered at around 2.34 Å with a 0.3 Å full width at half maximum value (FWHM) represents the Si—Si bond length distribution in NC (Fig. 2 inset). The maximum extent of the NC can also be read from same plot at about 27 Å, where the RDF goes to zero. Observation of a broad first peak in Fig. 2 demands further investigation of Si—Si RDF of NC atoms. For this purpose, in Fig. 3 we present bond length probability distributions (akin to RDF) for three categories of Si atoms: inner-core (with no bonds to surface atoms), outer-core (bonded to the surface), and surface NC atoms. We observe from Fig. 3 that Si—Si bond lengths in the inner core are centered around the equilibrium value and have a narrow width due mainly to thermal vibrations, whereas the bond length distributions of outer-core and surface atoms have increasing shifts for the most probable bond length values and broader widths. These shifts, and particularly, the increase in distribution widths cannot be attributed to thermal broadening. Taken together, these two observations is a clear indication of increasing strain as a function of distance from the center of the NC. To further investigate this deviation of Si—Si bonds from crystalline Si, in Fig. 4 we present bond length distribution with respect to the distance to the NC surface averaged over 2 ps of simulation time after the steady state is reached. This figure illustrates the gradual development of radial strain from the center to the NC surface. These observations show clearly that oxidation at the
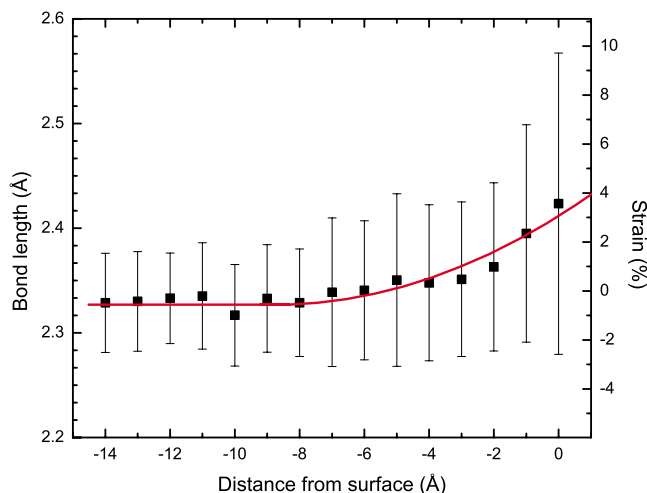

FIG. 4. (Color online) Variation of Si—Si bond length averages (calculated over 1 Å wide bins) as a function of distance from the NC surface, which is defined by Delaunay tesselation. The solid line is a fit to the data to guide the eye.

surface of NC results in a tensile strain at Si—Si bonds, which becomes significant only around the interface, while keeping the inner core almost unstrained. This tensile strain in the NC agrees with previous measurements of Hofmeister *et al.*[16]

Another consequence of this tensile strain is that the total bond orders of core-NC atoms are somewhat smaller than those of oxide Si, as seen in Fig. 5. In the same figure, we also show the calculated net charges using the electron equilibration method.[17] Nearly zero net charges of the core-Si atoms reflect the covalent type of bonding well within the NC. The bonding becomes increasingly ionic away from the NC core, as observed by the charges of Si
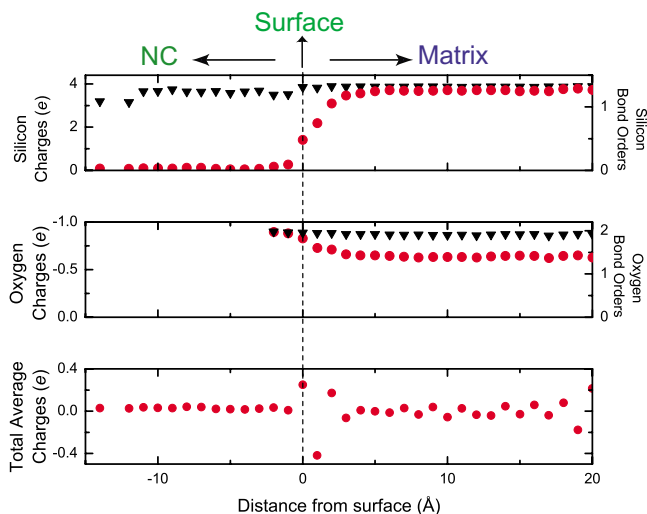

FIG. 5. (Color online) Top: Silicon bond orders (triangles) and charges (circles) as functions of distance from the surface of NC. Middle: Oxygen bond orders and charges as functions of distance from the surface of NC. Bottom: Total average charge as a function of distance from the surface of NC. The averaging bin width is 1 Å.

TABLE I. Statistical results of atom charges and numbers N for all NC diameters D_{NC} considered. The abbreviations for atom types are explained in Fig. 1. Charges are in the units of electronic charge and the angles θ are in degrees.

D_{NC} (Å)	N_c	N_s	N_O	ss			sm		ssm			sss		mms	
				N_{ss}	Charge	θ_{ss}	N_{ss}	Charge	N_{ssm}	Charge	θ_{ss}	N_{sss}	Charge	N_{mms}	Charge
11.0	10	25	32	2	−0.88	169.7	24	−0.76	5	−0.74	97.0	0		1	−0.81
15.4	42	42	59	5	−0.77	136.1	51	−0.74	1	−0.73	82.7	0		2	−0.77
18.0	83	62	77	11	−0.82	120.5	56	−0.74	1	−0.83	141.2	0		9	−0.79
19.8	114	76	82	14	−0.82	139.3	49	−0.73	4	−0.81	123.1	1	−0.85	14	−0.79
26.8	353	143	170	20	−0.81	118.0	123	−0.74	11	−0.79	120.9	0		15	−0.76
30.8	558	203	243	35	−0.83	123.9	159	−0.74	10	−0.80	115.9	2	−0.80	34	−0.79
33.4	718	238	268	44	−0.83	123.0	179	−0.75	18	−0.80	125.7	4	−0.84	23	−0.78

atoms, which reach the value of $1.3e$ at the oxide region (Fig. 5). As a result, the positive charges of surface-Si atoms form a shell at the surface of NC. This observation is similar to those obtained with DFT calculations.[18,19] On the other hand, negative charges of oxygen atoms bonded to the surface form another shell that encloses NC, and, finally, total average charges approach to zero within the oxide region. In Fig. 5, we also observe that the magnitude of the average charges of oxygen atoms that are bonded to the surface is greater than that in the matrix. However, the bond orders are nearly the same. This is due to the existence of 3cO atoms bonded to the surface. Note that the average bond order of oxygen atoms that are bonded to the surface is about 2 (see Fig. 5). Thus, those oxygen atoms form three partial bonds, two strong bonds and one weak bond. Finally, we would like to note that unlike many others,[2,3,6] we do not observe any double bonds.

The occurrence of 3cO has been noted by a number of groups. Pasquarello showed that the bistable E'_1 defect of an α-quartz structure may lead to 3cO as a metastable state as well as a Si—Si dimer bond and calculated the energy of the former to be higher than the latter. Pasquarello proposed that 3cO acts as an *intermediate metastable state* during structural relaxations at the interface.[20] Similarly, Boero *et al.* observed 3cO atoms in their *ab initio* calculations[21] and reported this feature as a metastable state. In Table I, we present the collected statistical data at the end of the simulation for 75 ps. For all oxygen complexes, the number of bridges, average charges of bridge oxygens, and average bridge angles for s-O-s are tabulated. We observe in Table I that the number of sss complexes is very small due to the narrow bond angle requirement of this configuration. For the remaining 3cO complexes, ssm and mms, their percentages are seen to increase with curvature. This can explain the fact that other studies[20,21] that have identified the 3cO complexes as metastable were based on the *planar* Si/SiO$_2$ interfaces. So, this is an indication of the importance of curvature in the stability of 3cO complexes. Hence, as one would expect, there is a linear relation between the total number of bridges with surface area, as indicated in Fig. 6. This finding is supported by Kroll and Schulte, who reported 3 and 33 such bridges for Si NC with radii 4.30 and 7.0 Å, respectively.[18]

IV. CONCLUSIONS

In conclusion, the realistic chemical environment provided by the reactive force field model enables us to understand the bond topology of the Si NC/a-SiO$_2$ interface and its internal dynamics. Particularly, it reveals that there are different types of oxygen complexes at the Si NC surface, some of which contain 3cO complexes whereas there are no double bonds. The curvature has a positive effect on the occurence of 3cO. The relative abundance of different complexes and their charge and geometrical characteristics are extracted. The inner core is observed to be almost unstrained, while the outer core and the interface region of the NC are under increasing strain up to about a few percent. In general, our work clearly shows that the Si NC–oxide interface is more complicated than the previously proposed schemes, which were based on solely simple bridge and double bonds. The provided information here paves the way to constructing realistic Monte Carlo moves for the simulation of large-scale silicon nanostructures embedded in an oxide matrix.
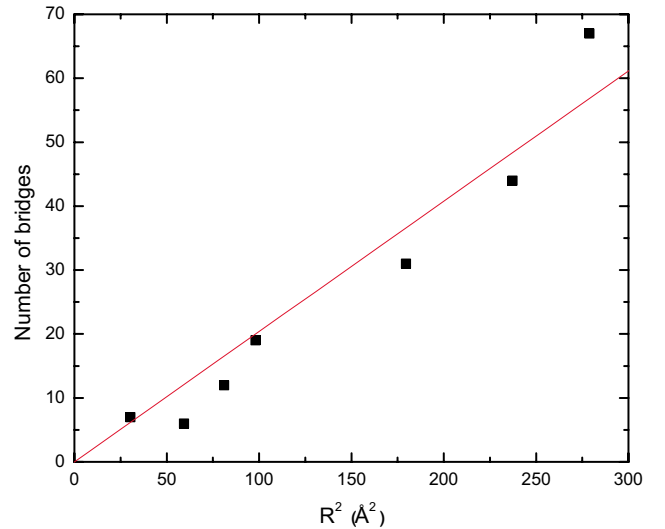

FIG. 6. (Color online) The number of bridges at the Si NC surface vs radius squared. The line is a linear fit to the data.

*dundar@fen.bilkent.edu.tr

†bulutay@fen.bilkent.edu.tr

‡cagin@chemail.tamu.edu

[1] T. Canham, Appl. Phys. Lett. **57**, 1046 (1990).

[2] M. V. Wolkin, J. Jorne, P. M. Fauchet, G. Allan, and C. Delerue, Phys. Rev. Lett. **82**, 197 (1999).

[3] A. Puzder, A. J. Williamson, J. C. Grossman, and G. Galli, Phys. Rev. Lett. **88**, 097401 (2002).

[4] E. Luppi, F. Iori, R. Magri, O. Pulci, S. Ossicini, E. Degoli, and V. Olevano, Phys. Rev. B **75**, 033303 (2007).

[5] M. Gatti and G. Onida, Phys. Rev. B **72**, 045442 (2005).

[6] I. Vasiliev, J. R. Chelikowsky, and R. M. Martin, Phys. Rev. B **65**, 121302(R) (2002).

[7] Y. Tu and J. Tersoff, Phys. Rev. Lett. **89**, 086102 (2002).

[8] G. Hadjisavvas and P. C. Kelires, Phys. Rev. Lett. **93**, 226104 (2004).

[9] D. E. Yılmaz, C. Bulutay, and T. Çağın, J. Nanosci. Nanotechnol. **8**, 635 (2008).

[10] A. Pasquarello, M. S. Hybertsen, and R. Car, Nature (London) **395**, 58 (1998).

[11] D. W. Brenner, Phys. Rev. B **42**, 9458 (1990); D. W. Brenner, O. A. Shenderova, J. A. Harrison, S. J. Stuart, B. Ni, and S. B. Sinnot, J. Phys.: Condens. Matter **14**, 783 (2002).

[12] A. C. T. van Duin, A. Strachan, S. Stewman, Q. Zhang, X. Xu, and W. A. Goddard III, J. Phys. Chem. A **107**, 3803 (2003).

[13] E. Demiralp, T. Çağın, and W. A. Goddard, Phys. Rev. Lett. **82**, 1708 (1999).

[14] N. T. Huff, E. Demiralp, T. Çağın, and W. A. Goddard, J. Non-Cryst. Solids **253**, 133 (1999).

[15] R. J. Renka, ACM Trans. Math. Softw. **22**, 1 (1996).

[16] H. Hofmeister, F. Huisken, and B. Kohn, Eur. Phys. J. D **9**, 137 (1999).

[17] A. K. Rappe and W. A. Goddard, J. Phys. Chem. **95**, 3358 (1991).

[18] P. Kroll and H. J. Schulte, Phys. Status Solidi B **243**, R47 (2006).

[19] P. Kroll and H. J. Schulte, Mater. Res. Soc. Symp. Proc. **958**, 0958L07 (2007).

[20] A. Pasquarello, Appl. Surf. Sci. **166**, 451 (2000).

[21] M. Boero, A. Oshiyama, P. L. Silvestrelli, and K. Murakami, Appl. Phys. Lett. **86**, 201910 (2005).